Generalized Power Iteration-based Precoding with Low-Complexity Matrix Inversion Approaches for Massive MIMO Systems

Mintaek Oh, Seunghyeong Yoo, Namyoon Lee, and Jinseok Choi

Abstract—**Generalized power iteration-based precoding (GPIP) exhibits superior performance in maximizing spectral efficiency for multi-antenna communications. Increasing the number of antennas, however, makes GPIP less practical due to its cubic complexity with respect to the number of antennas in computing matrix inversion. To resolve this, we propose efficient GPIP methods with imperfect channel knowledge. Exploiting the GPIP matrix structure, we use two low-complexity matrix inversion approaches: the matrix inversion lemma-based low-dimension matrix inversion and Gauss-Seidel iteration. These approaches decrease complexity order to the square of the number of antennas. Simulations validate the computational efficiency of the proposed methods while maintaining performance.**

Index Terms—**Massive MIMO, precoding, generalized power iteration, low-complexity, imperfect channel state information.**

I. INTRODUCTION

The surging demand for high-speed wireless communications has positioned massive multiple-input multiple-output (MIMO) systems as a cornerstone technology for next-generation wireless networks beyond 5G and into 6G [1]. Massive MIMO, which deploys a large number of antennas at the base station (BS), offers significant enhancements in spectral efficiency (SE), energy efficiency, and overall network capacity. However, realizing these benefits introduces substantial implementation challenges, particularly in the design and execution of precoding techniques [2].

Precoding in MIMO systems plays a crucial role in mitigating inter-user interference and maximizing system performance. In this regard, numerous studies have focused on developing high-performance precoding algorithms such as weighted minimum mean square error (WMMSE) [3] and generalized power iteration (GPI) [4], which have demonstrated superior capabilities in managing interference and maximizing beam gain. When perfect channel state information at the

transmitter (CSIT) is available, traditional zero-forcing (ZF) precoding is often sufficient in the medium to high signal-to-noise-ratio (SNR) regime. In practical scenarios where the BS has imperfect CSIT, however, the ZF precoder is no longer near-optimal. This limitation has led to extensive research into robust precoding techniques suitable for realistic conditions [5]. For example, the sample average approximation (SAA) technique in [6] was applied to the WMMSE algorithm to account for CSIT estimation errors in which the WMSEs are approximated by their empirical average. In addition, it was shown that GPI-based precoding (GPIP) offers robust precoding based on an error covariance-embedded metric [4].

While WMMSE-based precoding approaches often require an optimization toolbox (e.g. CVX) [6], GPIP approaches have garnered significant attention due to its toolbox-free operation and consistently superior performance across various communication scenarios [4], [7], [8]. Although the computational complexity of GPIP is relatively low, it increases cubically with the number of antennas $O(N^3)$ in a general case, which makes it less practical with larger N. Consequently, in massive MIMO systems, where N can range from tens to hundreds of antennas, there is a clear need to develop computationally efficient GPIP approaches that maintain high-performance while reducing complexity. Moreover, several recent studies have explored low-complexity precoding techniques designed for large-scale MIMO systems [9], [10]. These motivate us to present computationally efficient GPIP methods for massive MIMO systems under the imperfect CSIT assumption.

In this work, we propose low-complex matrix inversion-based GPIP methods for massive MIMO systems with imperfect CSIT. We first approximate the channel error covariance matrices with their principal eigen components. Then, leveraging the special structure of a GPIP matrix, we apply the matrix inversion lemma to reduce the overall complexity from $O(N^3)$ to $O(N^2)$ with respect to the number of the transmit antennas. This approach is particularly more effective for channels with a low-rank channel estimation error covariance matrix in terms of reducing the computation time of the algorithm. For a high-rank case, we further put forth an iterative refinement approach based on the Gauss-Seidel (GS) method, which also achieves $O(N^2)$ complexity with respect to N with marginal additional iterations. Via numerical evaluation, we validate that our proposed algorithms achieve significant complexity reduction with large N while maintaining comparable performance to the existing GPIP under the imperfect CSIT assumption.

Notation: $\mathbf{I}_N$ is the identity matrix of size $N \times N$ and

$\mathbf{0}$ is a zero vector with proper dimension. Assuming that $\mathbf{A}_1, \ldots, \mathbf{A}_N \in \mathbb{C}^{K \times K}$, $\mathbf{A} = \text{blkdiag}(\mathbf{A}_1, \ldots, \mathbf{A}_N) \in \mathbb{C}^{KN \times KN}$ is a block diagonal matrix. $\|\mathbf{a}\|$ and $\|\mathbf{A}\|_F$ represent L2 norm and Frobenius norm. We use $\text{vec}(\cdot)$ for vectorization and $\text{rank}(\cdot)$ for rank of a matrix. With mean m and variance σ^2, we use $\mathcal{CN}(m, \sigma^2)$ for a circularly symmetric complex Gaussian distribution.

II. System Model & Problem Formulation

A. System Model

We consider a single-cell downlink massive MIMO systems where the BS with N antennas serves K single-antenna users ($K \ll N$). Each user's data symbol s_k is drawn from a zero-mean Gaussian distribution with variance P (i.e., $\mathbb{E}[|s_k|^2] = P$). The BS transmits these symbols using a linear precoder $\mathbf{F} = [\mathbf{f}_1, \ldots, \mathbf{f}_K] \in \mathbb{C}^{N \times K}$, where $\mathbf{f}_k$ is the precoding vector for s_k. A transmitted signal vector $\mathbf{x} \in \mathbb{C}^N$ is given by

$$\mathbf{x} = \mathbf{Fs}, \tag{1}$$

where $\mathbf{s} = [s_1, \ldots, s_K]^\top \in \mathbb{C}^K$. The received signal of user k is given by $y_k = \mathbf{h}_k^\mathsf{H} \mathbf{f}_k s_k + \sum_{\ell \neq k, \ell=1}^K \mathbf{h}_k^\mathsf{H} \mathbf{f}_\ell s_\ell + n_k$, where $\mathbf{h}_k \in \mathbb{C}^N$ is a channel vector between the BS and user k, and $n_k \sim \mathcal{CN}(0, \sigma^2)$ is an additive white Gaussian noise.

The estimated CSIT is given as

$$\hat{\mathbf{h}}_k = \mathbf{h}_k - \mathbf{e}_k, \tag{2}$$

where $\mathbf{e}_k$ is the corresponding channel estimation error vector with its covariance matrix $\mathbb{E}[\mathbf{e}_k \mathbf{e}_k^\mathsf{H}] = \mathbf{\Psi}_k$. We assume that $\hat{\mathbf{h}}_k$ and $\mathbf{\Psi}_k$, $\forall k$, are available at the BS.

B. Problem Formulation

With our system model, the SE of user k is defined as

$$R_k = \log_2\left(1 + \frac{|\mathbf{h}_k^\mathsf{H} \mathbf{f}_k|^2}{\sum_{i=1, i \neq k}^K |\mathbf{h}_k^\mathsf{H} \mathbf{f}_i|^2 + \frac{\sigma^2}{P}}\right). \tag{3}$$

We note that the SE in (3) requires the perfect CSIT. Accordingly, it is necessary to closely express the SE in (3) without the perfect CSIT but only with the given channel knowledge, i.e., $\hat{\mathbf{h}}_k$ and $\mathbf{\Psi}_k$. To this end, we define the instantaneous SE that captures the short-term SE by considering channel estimation errors in each realization. According to [6], the ergodic SE of user k in a given fading block is given as

$$\mathbb{E}_{\{\mathbf{h}_k\}}[R_k] = \mathbb{E}_{\{\hat{\mathbf{h}}_k\}}\left[\mathbb{E}_{\{\mathbf{h}_k | \hat{\mathbf{h}}_k\}}[R_k | \hat{\mathbf{h}}_k]\right] = \mathbb{E}_{\{\hat{\mathbf{h}}_k\}}[R_k^{\text{ins}}], \tag{4}$$

where the expectation is taken over the uncertainty a in the channel fading process, and R_k^{ins} denotes the instantaneous SE:

$$R_k^{\text{ins}} = \mathbb{E}_{\{\mathbf{e}_k\}}\left[\log_2\left(1 + \frac{|\mathbf{h}_k^\mathsf{H} \mathbf{f}_k|^2}{\sum_{i=1, i \neq k}^K |\mathbf{h}_k^\mathsf{H} \mathbf{f}_i|^2 + \frac{\sigma^2}{P}}\right)\bigg| \hat{\mathbf{h}}_k\right]. \tag{5}$$

Considering independent and identically distributed Gaussian channel estimation errors with proper bounding, the lower bound of the instantaneous SE $\bar{R}_k^{\text{ins}}$ is derived as [4]

$$R_k^{\text{ins}} \geq \log_2\left(1 + \frac{|\mathbf{h}_k^\mathsf{H} \mathbf{f}_k|^2}{\sum_{i=1, i \neq k}^K |\mathbf{h}_k^\mathsf{H} \mathbf{f}_i|^2 + \sum_{i=1}^K \mathbf{f}_i^\mathsf{H} \mathbf{\Psi}_k \mathbf{f}_i + \frac{\sigma^2}{P}}\right) = \bar{R}_k^{\text{ins}}. \tag{6}$$

Using (6), we can formulate the more effective SE maximization problem under imperfect CSIT with $\hat{\mathbf{h}}_k$ and $\mathbf{\Psi}_k$ as

$$\underset{\mathbf{f}_1, \cdots, \mathbf{f}_K}{\text{maximize}} \sum_{k=1}^K \bar{R}_k^{\text{ins}} \tag{7}$$

$$\text{subject to} \sum_{k=1}^K \|\mathbf{f}_k\|^2 \leq 1. \tag{8}$$

Since this problem is inherently non-convex with respect to the precoder, it is infeasible to identify globally optimal solution.

III. Low-Complexity Matrix Inversion GPIP

A. Preliminaries: GPIP Algorithm

In this section, we briefly explain the GPIP method [4]. To solve (7), we first vectorize the precoding matrix as

$$\bar{\mathbf{f}} = \text{vec}(\mathbf{F}) = [\mathbf{f}_1^\top, \mathbf{f}_2^\top, \ldots, \mathbf{f}_K^\top]^\top \in \mathbb{C}^{NK}. \tag{9}$$

Considering the maximum power transmission with P, we set $\|\bar{\mathbf{f}}\|^2 = 1$ to achieve the maximum sum SE. Subsequently, we replace $\frac{\sigma^2}{P}$ with $\frac{\sigma^2}{P}\|\mathbf{f}\|^2$ in (6), and transform the objective function in (7) to the function of Rayleigh quotient forms as

$$\underset{\bar{\mathbf{f}}}{\text{maximize}} \sum_{k=1}^K \log_2\left(\frac{\bar{\mathbf{f}}^\mathsf{H} \mathbf{A}_k \bar{\mathbf{f}}}{\bar{\mathbf{f}}^\mathsf{H} \mathbf{B}_k \bar{\mathbf{f}}}\right), \tag{10}$$

where

$$\mathbf{A}_k = \text{blkdiag}\left(\hat{\mathbf{h}}_k \hat{\mathbf{h}}_k^\mathsf{H} + \mathbf{\Psi}_k, \cdots, \hat{\mathbf{h}}_k \hat{\mathbf{h}}_k^\mathsf{H} + \mathbf{\Psi}_k\right) + \mathbf{I}_{NK} \frac{\sigma^2}{P}, \tag{11}$$

$$\mathbf{B}_k = \mathbf{A}_k - \text{blkdiag}\left(\mathbf{0}, \cdots, \hat{\mathbf{h}}_k \hat{\mathbf{h}}_k^\mathsf{H}, \cdots, \mathbf{0}\right). \tag{12}$$

We can ignore the transmit power constraint (8) because of $\|\bar{\mathbf{f}}\|^2 = 1$ and scaling invariance of (10) for $\bar{\mathbf{f}}$. For simplicity, we define the objective function in (10) as

$$\mathcal{L}(\bar{\mathbf{f}}) = \log_2 \prod_{k=1}^K \left(\frac{\bar{\mathbf{f}}^\mathsf{H} \mathbf{A}_k \bar{\mathbf{f}}}{\bar{\mathbf{f}}^\mathsf{H} \mathbf{B}_k \bar{\mathbf{f}}}\right) = \log_2 \mu(\bar{\mathbf{f}}). \tag{13}$$

Then, we derive Lemma 1 to find the stationary points of (13).

Lemma 1. *The stationarity condition of the problem in* (10) *is satisfied if*

$$\bar{\mathbf{B}}^{-1}(\bar{\mathbf{f}}) \bar{\mathbf{A}}(\bar{\mathbf{f}}) \bar{\mathbf{f}} = \mu(\bar{\mathbf{f}}) \bar{\mathbf{f}}, \tag{14}$$

where

$$\bar{\mathbf{A}}(\bar{\mathbf{f}}) = \sum_{k=1}^K \frac{\mathbf{A}_k}{\bar{\mathbf{f}}^\mathsf{H} \mathbf{A}_k \bar{\mathbf{f}}} \mu_{\text{num}}(\bar{\mathbf{f}}), \quad \bar{\mathbf{B}}(\bar{\mathbf{f}}) = \sum_{k=1}^K \frac{\mathbf{B}_k}{\bar{\mathbf{f}}^\mathsf{H} \mathbf{B}_k \bar{\mathbf{f}}} \mu_{\text{den}}(\bar{\mathbf{f}}). \tag{15}$$

Here, $\mu_{\text{num}}(\bar{\mathbf{f}})$ and $\mu_{\text{den}}(\bar{\mathbf{f}})$ can be any function such that $\mu(\bar{\mathbf{f}}) = \mu_{\text{num}}(\bar{\mathbf{f}})/\mu_{\text{den}}(\bar{\mathbf{f}})$.

Proof. Please refer to the proof of Lemma 1 in [4]. ∎

The stationarity condition in (10) can be viewed as a generalized eigenvalue problem, where $\mu(\bar{\mathbf{f}})$ is an eigenvalue of $\bar{\mathbf{B}}^{-1}(\bar{\mathbf{f}}) \bar{\mathbf{A}}(\bar{\mathbf{f}})$ with $\bar{\mathbf{f}}$ as its eigenvector. Consequently, maximizing the objective $\mathcal{L}(\bar{\mathbf{f}})$ is equivalent to maximizing $\mu(\bar{\mathbf{f}})$, which involves finding the principal eigenvalue of (10) corresponding to the superior local optimum of (7). Based on this formulation, GPIP [4] is described in Algorithm 1.

Algorithm 1: GPIP

---

1 **initialize**: $\mathbf{F}^{(0)}$.
2 Set $\bar{\mathbf{f}}^{(0)} = \text{vec}(\mathbf{F}^{(0)})$ and $t = 1$.
3 **while** $\left\| \bar{\mathbf{f}}^{(t)} - \bar{\mathbf{f}}^{(t-1)} \right\| > \varepsilon$ & $t \le t_{\max}$ **do**
4   Compute $\bar{\mathbf{A}}(\bar{\mathbf{f}}^{(t-1)})$ and $\bar{\mathbf{B}}(\bar{\mathbf{f}}^{(t-1)})$ by (15).
5   Compute $\bar{\mathbf{f}}^{(t)} = \bar{\mathbf{B}}^{-1}(\bar{\mathbf{f}}^{(t-1)})\bar{\mathbf{A}}(\bar{\mathbf{f}}^{(t-1)})\bar{\mathbf{f}}^{(t-1)}$.
6   Normalize $\bar{\mathbf{f}}^{(t)} = \bar{\mathbf{f}}^{(t)}/\left\|\bar{\mathbf{f}}^{(t)}\right\|$.
7     $t \leftarrow t + 1$.
8 **return** $\bar{\mathbf{f}}^{\star} \leftarrow \bar{\mathbf{f}}^{(t)}$.

Remark 1. The primary computational burden in Algorithm 1 comes from calculating matrix inversion of $\bar{\mathbf{B}}(\bar{\mathbf{f}})$. Since $\bar{\mathbf{B}}(\bar{\mathbf{f}})$ is block-diagonal and Hermitian, we need $O(KN^3)$ for computing $\bar{\mathbf{B}}^{-1}(\bar{\mathbf{f}})$ [4]. Hence, the overall complexity of Algorithm 1 is $O(TKN^3)$ where T is the number of iterations. The cubic dependency on N poses a significant challenge for large-scale antenna systems. To alleviate this bottleneck, we propose the computationally efficient GPIP approaches in the sequel.

B. Low-Dimensional Matrix Inversion Approach

We first introduce our low-complexity matrix inversion-based GPIP algorithm by using a low-dimensional matrix inversion approach, which is called LD-GPIP. To this end, we first divide $\bar{\mathbf{B}}(\bar{\mathbf{f}})$ by $\mu_{\text{den}}(\bar{\mathbf{f}})$ in (15), i.e., $\widehat{\mathbf{B}}(\mathbf{f}) = \bar{\mathbf{B}}(\bar{\mathbf{f}})/\mu_{\text{den}}(\bar{\mathbf{f}})$, which does not affect the direction of the precoding vector due to the normalization in Algorithm 1. We then leverage the special structure of the GPI matrix $\bar{\mathbf{B}}(\bar{\mathbf{f}})$: from (15), we can define kth sub-block matrix of $\widehat{\mathbf{B}}(\bar{\mathbf{f}})$ as

$$\bar{\mathbf{B}}_k^{\text{sub}}(\bar{\mathbf{f}}) = \alpha(\bar{\mathbf{f}})\left(\beta(\bar{\mathbf{f}})\sum_{j \ne k} b_j(\bar{\mathbf{f}})\hat{\mathbf{h}}_j\hat{\mathbf{h}}_j^{\mathsf{H}} + \sum_{i=1}^{K} b_i(\bar{\mathbf{f}})\boldsymbol{\Psi}_i + \mathbf{I}_N\right), \quad (16)$$

where $b_i(\bar{\mathbf{f}}) = \frac{1}{\bar{\mathbf{f}}^{\mathsf{H}}\mathbf{B}_i\bar{\mathbf{f}}}$, $\alpha(\bar{\mathbf{f}}) = \frac{\sigma^2}{P}\sum_{\ell=1}^{K} b_\ell(\bar{\mathbf{f}})$, $\beta(\bar{\mathbf{f}}) = 1/\alpha(\bar{\mathbf{f}})$.

We apply low-rank approximation to the error covariance matrix as

$$\boldsymbol{\Psi}_k \approx \sum_{\ell=1}^{r_k} \lambda_{\ell,k}\boldsymbol{\psi}_{\ell,k}\boldsymbol{\psi}_{\ell,k}^{\mathsf{H}}, \quad (17)$$

where r_k is an arbitrary integer value satisfying $0 \le r_k \le \text{rank}(\boldsymbol{\Psi}_k)$, $\lambda_{\ell,k}$ is an ℓth eigenvalue, and $\boldsymbol{\psi}_{\ell,k}$ is an ℓth eigenvector of $\boldsymbol{\Psi}_k$. For simplicity, we assume $r = r_k, \forall k$. According to Eckart–Young–Mirsky theorem [11], the error bound of the low-rank approximation is given by

$$\left\|\boldsymbol{\Psi}_k - \tilde{\boldsymbol{\Psi}}_k\right\|_F^2 \ge \sum_{\ell=r_k+1}^{\text{rank}(\boldsymbol{\Psi})} \lambda_{\ell,k}^2, \quad (18)$$

where we assume that the eigenvalues of $\boldsymbol{\Psi}_k$ are arranged in descending order for all k. To achieve the lower bound, we can select the eigenvectors corresponding to the largest eigenvalues. Using (17), we can approximate (16) as

$$\bar{\mathbf{B}}_k^{\text{sub}}(\bar{\mathbf{f}}) \approx \tilde{\mathbf{B}}_k^{\text{sub}}(\bar{\mathbf{f}}) \quad (19)$$

$$= \alpha(\bar{\mathbf{f}})\left(\beta(\bar{\mathbf{f}})\sum_{j \ne k} b_j(\bar{\mathbf{f}})\hat{\mathbf{h}}_j\hat{\mathbf{h}}_j^{\mathsf{H}} + \sum_{i=1}^{K}\sum_{\ell=1}^{r} b_i(\bar{\mathbf{f}})\lambda_{\ell,i}\boldsymbol{\psi}_{\ell,i}\boldsymbol{\psi}_{\ell,i}^{\mathsf{H}} + \mathbf{I}_N\right).$$

Hence, the overall approximated matrix is defined as $\tilde{\mathbf{B}}^{-1}(\bar{\mathbf{f}}) = \text{blkdiag}\left(\left[\tilde{\mathbf{B}}_1^{\text{sub}}(\bar{\mathbf{f}}^{(t-1)})\right]^{-1}, \cdots, \left[\tilde{\mathbf{B}}_K^{\text{sub}}(\bar{\mathbf{f}}^{(t-1)})\right]^{-1}\right)$.

To achieve low-dimensional matrix inversion, we first define

$$\mathbf{Z}(\bar{\mathbf{f}}) = \alpha(\bar{\mathbf{f}})\mathbf{I}_N + \mathbf{V}(\bar{\mathbf{f}})\mathbf{V}^{\mathsf{H}}(\bar{\mathbf{f}}), \quad (20)$$

where

$$\mathbf{V}(\mathbf{f}) = \left[\sqrt{b_1(\bar{\mathbf{f}})}\hat{\mathbf{h}}_1, \cdots, \sqrt{b_K(\bar{\mathbf{f}})}\hat{\mathbf{h}}_K, \boldsymbol{\Gamma}(\bar{\mathbf{f}})\right] \in \mathbb{C}^{N \times (K+rK)}, \quad (21)$$

and $\boldsymbol{\Gamma}(\mathbf{f}) = \left[\sqrt{b_1(\bar{\mathbf{f}})\lambda_{1,1}}\boldsymbol{\psi}_{1,1}, \cdots, \sqrt{b_K(\bar{\mathbf{f}})\lambda_{r,K}}\boldsymbol{\psi}_{r,K}\right] \in \mathbb{C}^{N \times rK}$. Then, we apply the matrix inversion lemma called *Sherman-Morrison-Woodbury (SMW) formula* [12] $\left(\mathbf{A} + \mathbf{U}\mathbf{V}^{\mathsf{H}}\right)^{-1} = \mathbf{A}^{-1} - \mathbf{A}^{-1}\mathbf{U}(\mathbf{I} + \mathbf{V}^{\mathsf{H}}\mathbf{A}^{-1}\mathbf{U})^{-1}\mathbf{V}^{\mathsf{H}}\mathbf{A}^{-1}$ to (20):

$$\mathbf{Z}^{-1}(\bar{\mathbf{f}}) = \left(\alpha(\bar{\mathbf{f}})\mathbf{I}_N + \mathbf{V}(\bar{\mathbf{f}})\mathbf{V}^{\mathsf{H}}(\bar{\mathbf{f}})\right)^{-1}$$

$$= \beta(\bar{\mathbf{f}})\left[\mathbf{I}_N - \beta(\bar{\mathbf{f}})\mathbf{V}(\bar{\mathbf{f}})\left(\mathbf{I}_{\bar{r}K} + \beta(\bar{\mathbf{f}})\mathbf{V}^{\mathsf{H}}(\bar{\mathbf{f}})\mathbf{V}(\bar{\mathbf{f}})\right)^{-1}\mathbf{V}^{\mathsf{H}}(\bar{\mathbf{f}})\right], \quad (22)$$

where $\bar{r} = 1 + r$. Accordingly, we need the $\bar{r}K \times \bar{r}K$ matrix inversion as shown in (22) instead of $N \times N$ matrix inversion for computing $\mathbf{Z}^{-1}(\bar{\mathbf{f}})$. Noting $\tilde{\mathbf{B}}_k^{\text{sub}}(\bar{\mathbf{f}}) = \mathbf{Z}(\bar{\mathbf{f}}) - b_k(\bar{\mathbf{f}})\hat{\mathbf{h}}_k\hat{\mathbf{h}}_k^{\mathsf{H}}$, the inverse of $\tilde{\mathbf{B}}_k^{\text{sub}}(\bar{\mathbf{f}})$ is computed as

$$\left[\tilde{\mathbf{B}}_k^{\text{sub}}(\bar{\mathbf{f}})\right]^{-1} = \left(\mathbf{Z}(\bar{\mathbf{f}}) - b_k(\bar{\mathbf{f}})\hat{\mathbf{h}}_k\hat{\mathbf{h}}_k^{\mathsf{H}}\right)^{-1}$$

$$\overset{(a)}{=} \mathbf{Z}^{-1}(\bar{\mathbf{f}}) + \frac{b_k(\bar{\mathbf{f}})\mathbf{Z}^{-1}(\bar{\mathbf{f}})\hat{\mathbf{h}}_k\hat{\mathbf{h}}_k^{\mathsf{H}}\mathbf{Z}^{-1}(\bar{\mathbf{f}})}{1 - b_k(\bar{\mathbf{f}})\hat{\mathbf{h}}_k^{\mathsf{H}}\mathbf{Z}^{-1}(\bar{\mathbf{f}})\hat{\mathbf{h}}_k}, \quad (23)$$

where (a) comes from the *SMW formula*.

To understand LD-GPIP's behavior regarding SNR, we analyze the approximation error between $\bar{\mathbf{B}}^{-1}(\bar{\mathbf{f}})$ and $\tilde{\mathbf{B}}^{-1}(\bar{\mathbf{f}})$. Letting $\tilde{\mathbf{B}}(\bar{\mathbf{f}}) = \bar{\mathbf{B}}(\bar{\mathbf{f}}) + \mathbf{E}(\bar{\mathbf{f}})$, where $\mathbf{E}(\bar{\mathbf{f}})$ represents the error from using r eigenvectors in the low-rank approximation, i.e., $\mathbf{E}(\bar{\mathbf{f}}) = \text{blkdiag}\left(\mathbf{E}_1^{\text{sub}}(\bar{\mathbf{f}}), \cdots, \mathbf{E}_K^{\text{sub}}(\bar{\mathbf{f}})\right)$ with

$$\mathbf{E}_k^{\text{sub}}(\bar{\mathbf{f}}) = \alpha(\bar{\mathbf{f}})\sum_{i=1}^{K} b_i(\bar{\mathbf{f}})\left(\sum_{\ell=1}^{r_k} \lambda_{\ell,k}\boldsymbol{\psi}_{\ell,k}\boldsymbol{\psi}_{\ell,k}^{\mathsf{H}} - \boldsymbol{\Psi}_i\right), \quad (24)$$

we can derive the following relationship:

$$\tilde{\mathbf{B}}^{-1}(\bar{\mathbf{f}}) - \bar{\mathbf{B}}^{-1}(\bar{\mathbf{f}}) = -\bar{\mathbf{B}}^{-1}(\bar{\mathbf{f}})\mathbf{E}(\bar{\mathbf{f}})\tilde{\mathbf{B}}^{-1}(\bar{\mathbf{f}}). \quad (25)$$

This leads to the error bound by applying the sub-multiplicative property of the Frobenius norm:

$$\left\|\tilde{\mathbf{B}}^{-1}(\bar{\mathbf{f}}) - \bar{\mathbf{B}}^{-1}(\bar{\mathbf{f}})\right\|_F \le \left\|\tilde{\mathbf{B}}^{-1}(\bar{\mathbf{f}})\right\|_F \left\|\mathbf{E}(\bar{\mathbf{f}})\right\|_F \left\|\bar{\mathbf{B}}^{-1}(\bar{\mathbf{f}})\right\|_F. \quad (26)$$

Since $\alpha(\bar{\mathbf{f}}) = \frac{\sigma^2}{P}\sum_{\ell=1}^{K} b_\ell(\bar{\mathbf{f}})$, the right-hand side in (26) scales approximately as $1/\alpha(\bar{\mathbf{f}}) \propto \text{SNR}$ in the high SNR regime.

Given $\mathbf{Z}^{-1}(\bar{\mathbf{f}})$, each sub-matrix inversion in (23) has a complexity of $O(N^2)$, and the complexity of computing $\mathbf{Z}^{-1}(\bar{\mathbf{f}})$ from (22) is $O(\bar{r}^3K^3 + \bar{r}^2K^2N + \bar{r}KN^2)$. Therefore, the overall complexity of LD-GPIP is $O(T(\bar{r}^3K^3 + \bar{r}^2K^2N + \bar{r}KN^2))$. Such an indirect computation of $\left[\tilde{\mathbf{B}}_k^{\text{sub}}(\bar{\mathbf{f}})\right]^{-1}$ allows to avoid the need to repeatedly compute each matrix inversion of $\tilde{\mathbf{B}}_k^{\text{sub}}(\bar{\mathbf{f}})$, $\forall k$, with directly applying the *SMW formula* similarly as (22), which requires $O(TK(\bar{r}^3K^3 + \bar{r}^2K^2N + \bar{r}KN^2))$. This complexity is $K\times$ higher complexity than our indirect approach. In

---

Algorithm 2: LD-GPIP and GS-GPIP Algorithms

---

1 **initialize**: $\mathbf{F}^{(0)}$.
2 Set $\bar{\mathbf{f}}^{(0)} = \text{vec}(\mathbf{F}^{(0)})$ and $t = 1$.
3 **while** $\left\|\bar{\mathbf{f}}^{(t)} - \bar{\mathbf{f}}^{(t-1)}\right\| > \varepsilon \;\&\; t \leq t_{\max}$ **do**
4   **LD-GPIP**
5   Build $\bar{\mathbf{A}}(\bar{\mathbf{f}}^{(t-1)})$ and $\mathbf{Z}^{-1}(\bar{\mathbf{f}}^{(t-1)})$ by (22).
6   **for** $k = 1$ to K **do**
7   Compute $\left[\tilde{\mathbf{B}}_k^{\mathsf{sub}}(\bar{\mathbf{f}}^{(t-1)})\right]^{-1}$ by (23).
8   Update $\bar{\mathbf{f}}^{(t)} = \tilde{\mathbf{B}}^{-1}(\bar{\mathbf{f}}^{(t-1)})\bar{\mathbf{A}}(\bar{\mathbf{f}}^{(t-1)})\bar{\mathbf{f}}^{(t-1)}$.
9   **GS-GPIP**
10   Build $\bar{\mathbf{A}}(\bar{\mathbf{f}}^{(t-1)})$ and $\bar{\mathbf{B}}(\bar{\mathbf{f}}^{(t-1)})$ by (15).
11   **for** $\ell = 1$ to T_{GS} **do**
12   Compute $\bar{\mathbf{f}}^{\star(\ell)}$ by (29) with given $\bar{\mathbf{f}}^{(t-1)}$.
13   Update $\bar{\mathbf{f}}^{(t)} = \bar{\mathbf{f}}^{\star(\ell)}$.
14   Normalize $\bar{\mathbf{f}}^{(t)} = \bar{\mathbf{f}}^{(t)}/\left\|\bar{\mathbf{f}}^{(t)}\right\|$.
15    $t \leftarrow t + 1$.
16 **return** $\bar{\mathbf{f}}^{\star} \leftarrow \bar{\mathbf{f}}^{(t)}$.

---

addition, the complexity required for low-rank approximation in (17) for all K users is $O(rKN^2)$. This complexity is negligible since it needs to be performed only when $\boldsymbol{\Psi}_k$, the long-term statistics of the channel, changes.

Under perfect CSIT ($\bar{r} = 1$) or selecting a few eigenvectors, i.e., for $\bar{r}K \ll N$, the overall algorithm complexity nearly reduces to $O(T\bar{r}KN^2)$ which is much lower than the conventional complexity $O(TKN^3)$. In this regard, the proposed LD-GPIP can significantly reduce the complexity of GPIP for massive MIMO systems. This implies that although LD-GPIP works with any r, it is particularly more effective when $\boldsymbol{\Psi}_k$ can be well approximated with small r. Hence, to achieve high SE with $\boldsymbol{\Psi}_k$ which is well-conditioned and has higher rank, LD-GPIP exhibits the growing complexity. In this regard, we present another low-dimensional matrix inversion approach which can be applicable for a general $\boldsymbol{\Psi}_k$ with marginal additional iterations in the following subsection.

C. Iterative Refinement Approach

In this subsection, we propose an iterative refinement approach based on the *GS method* [13]. To this end, let us focus on the following update step in Algorithm 1:

$$\bar{\mathbf{f}}^{\star} = \bar{\mathbf{B}}^{-1}(\bar{\mathbf{f}})\bar{\mathbf{A}}(\bar{\mathbf{f}})\bar{\mathbf{f}}. \tag{27}$$

We decompose $\bar{\mathbf{B}}(\bar{\mathbf{f}})$ into a lower triangular matrix $\mathbf{L}(\bar{\mathbf{f}})$ and a strictly upper triangular matrix $\mathbf{U}(\bar{\mathbf{f}})$, i.e., $\bar{\mathbf{B}}(\bar{\mathbf{f}}) = \mathbf{L}(\bar{\mathbf{f}}) + \mathbf{U}(\bar{\mathbf{f}})$. The *GS method* then iteratively solves for the ℓ-th $\bar{\mathbf{f}}^{\star}$ by using its previous value on the right-hand side as

$$\bar{\mathbf{f}}^{\star(\ell)} = \mathbf{L}^{-1}(\bar{\mathbf{f}})\left(\bar{\mathbf{A}}(\bar{\mathbf{f}})\bar{\mathbf{f}} - \mathbf{U}(\bar{\mathbf{f}})\bar{\mathbf{f}}^{\star(\ell-1)}\right). \tag{28}$$

The solution in (28) is obtained through forward substitution, thereby eliminating the need for matrix inversion:

$$\left[\bar{\mathbf{f}}^{\star}\right]_i^{(\ell)} = \tag{29}$$

$$\frac{1}{\left[\bar{\mathbf{B}}(\bar{\mathbf{f}})\right]_{i,i}}\left(\left[\bar{\mathbf{A}}(\bar{\mathbf{f}})\bar{\mathbf{f}}\right]_i - \sum_{j<i}\left[\bar{\mathbf{B}}(\bar{\mathbf{f}})\right]_{i,j}\left[\bar{\mathbf{f}}^{\star}\right]_j^{(\ell)} - \sum_{j>i}\left[\bar{\mathbf{B}}(\bar{\mathbf{f}})\right]_{i,j}\left[\bar{\mathbf{f}}^{\star}\right]_j^{(\ell-1)}\right),$$

TABLE I
ALGORITHM COMPLEXITY FOR IMPERFECT CSIT ($\bar{r} = 1 + r$)

Algorithm	Overall Complexity
GPIP	$O(TKN^3)$
LD-GPIP	$O(T(\bar{r}^3K^3 + \bar{r}^2K^2N + \bar{r}KN^2))$
GS-GPIP	$O(T(T_{GS}KN^2))$

where $[\cdot]_{i,j}$ is the element in the ith row and jth column of a matrix and $[\cdot]_i$ is the ith element of a vector. The initial $\bar{\mathbf{f}}^{\star(0)}$ is determined as the existing $\bar{\mathbf{f}}$ before updating it with the *GS method*. By leveraging the block-diagonal structure of $\mathbf{L}(\bar{\mathbf{f}})$, the complexity of obtaining (28) with the forward substitution is reduced to $O(KN^2)$ instead of $O(K^2N^2)$. Consequently, the overall complexity of GS iteration-based GPIP, called GS-GPIP, is $O(T(T_{GS}KN^2))$ where T_{GS} is an inner iteration count.

We now analyze the convergence behavior of GS-GPIP. According to [13], the GS method converges whenever the underlying system matrix is symmetric positive definite (SPD). From (16), we confirm that $\bar{\mathbf{B}}(\bar{\mathbf{f}})$ is indeed SPD; therefore, the proposed GS-GPIP is guaranteed to converge. In [13], for $\bar{\mathbf{B}}(\bar{\mathbf{f}}) = \mathbf{M}(\bar{\mathbf{f}}) - \mathbf{N}(\bar{\mathbf{f}})$, its convergence rate is

$$\left\|\boldsymbol{\varepsilon}^{(\ell)}\right\| = O\left(\rho\left(\mathbf{M}(\bar{\mathbf{f}})^{-1}\mathbf{N}(\bar{\mathbf{f}})\right)^{\ell}\right), \tag{30}$$

where $\boldsymbol{\varepsilon}^{(\ell)} = \bar{\mathbf{f}}^{\star} - \bar{\mathbf{f}}^{\star(\ell)}$ and $\rho(\cdot)$ is the spectral radius that is the maximum of the absolute values of its eigenvalues.

Algorithm 2 presents our proposed method in which either LD-GPIP or GS-GPIP can be selected as the core update mechanism. In addition, we summarize the complexity orders of the considered GPIP-based algorithms in Table I. Compared to LD-GPIP, GS-GPIP scales linearly with K in terms of complexity. Therefore, GS-GPIP can be an attractive option for systems with a large number of users while maintaining $O(N^2)$ complexity.

IV. NUMERICAL RESULTS

In this section, we evaluate the sum SE and computational complexity of our proposed algorithms numerically. In the simulations, we consider the following algorithms:
- **GPIP**: The original GPIP algorithm [4].
- **GPIP (no Cov)**: The original GPIP algorithm without the error covariance-embedded metric (no use of $\boldsymbol{\Psi}_k$).
- **LD-GPIP**: The proposed GPIP in Section III-B.
- **GS-GPIP**: The proposed GPIP in Section III-C.
- **WMMSE-SAA**: The WMMSE precoder with SAA [6].
- **WMMSE**: The conventional WMMSE precoder [3].
- **FP**: A fractional programming (FP) precoder [14].
- **RZF**: A regularized zero forcing (RZF) precoder.

We use maximum ratio transmission as an initial precoder of the GPI-based algorithms, WMMSE, and FP. We set $t_{\max} = 20$ and $T_{GS} = 4$. For WMMSE-SAA, we use 10^3 samples for the SAA technique. To ensure fair comparison of computation times across different CSIT conditions, we allow all algorithms to run until they reach their maximum iteration counts. We assess computation time in MATLAB with the workstation equipped with i9-13900K CPU and 64GB RAM.

To generate the channel vector $\mathbf{h}_k$, we adopt a one-ring model [15] based on its spatial correlation matrix $\mathbf{R}_k =$

(a) $\Delta_k = \pi/20$, $r = 6$


(b) $\Delta_k = \pi/6$, $r = 15$
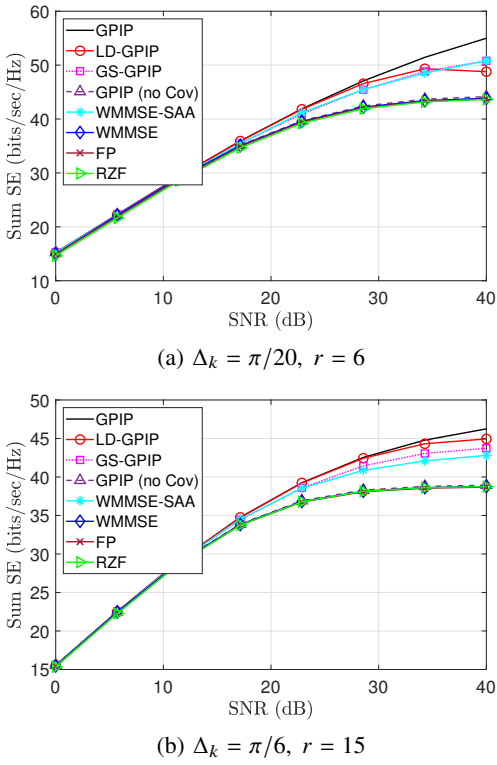
Fig. 1. The sum SE versus SNR for $N = 64$ BS antennas and $K = 4$ users.

TABLE II
COMPUTATIONAL TIME FOR FIG. 1 AT SNR = 30 dB (IN msec)

Algorithm	GPIP	LD-GPIP	GS-GPIP	WMMSE-SAA
Time (a)	52.2	**22.3**	28.0	39589.4
Time (b)	55.7	29.5	**27.6**	38632.0

$\mathbb{E}\left[\mathbf{h}_k \mathbf{h}_k^{\mathsf{H}}\right]$. Considering a time division duplex system with the linear minimum mean square error channel estimator [16], the channel error covariance matrix is given by

$$\boldsymbol{\Psi}_k = \mathbb{E}\left[\mathbf{e}_k \mathbf{e}_k^{\mathsf{H}}\right] = \mathbf{R}_k - \mathbf{R}_k \left(\mathbf{R}_k + \frac{\sigma^2}{\tau_{\mathsf{UL}}\rho_{\mathsf{UL}}}\mathbf{I}_N\right)^{-1}\mathbf{R}_k, \quad (31)$$

where τ_{UL} is uplink training length and ρ_{UL} is uplink training power for channel estimation. In this channel model, we uniformly generate AoAs of user k as $\theta_k \in (0, 2\pi]$, and consider $\tau_{\mathsf{UL}}\rho_{\mathsf{UL}} = 10$ and the predetermined r value.

We define the SNR as P/σ^2, and evaluate the performance of our proposed algorithms with respect to SNR for $N = 64$ and $K = 4$. For the kth user's angular spread Δ_k, we set two cases: (a) $\Delta_k = \pi/20$ for lower-rank channels with $r = 6$, and (b) $\Delta_k = \pi/6$ for higher-rank channels with $r = 15$, $\forall k$. In Fig. 1(a) and (b), our proposed algorithms offer substantial gain compared to other baselines while attaining similar SE performance with GPIP. In particular, at the high SNR (> 30 dB), Fig. 1(a) reveals a performance gap between LD-GPIP and GS-GPIP because LD-GPIP utilizes only $r = 6$ eigenvectors to approximate $\boldsymbol{\Psi}_k$. Meanwhile, in Fig. 1(b), LD-GPIP presents the higher SE than GS-GPIP in most SNR regime by considering enough $r = 15$. Nonetheless, GS-GPIP closely tracks the performance of GPIP with $T_{\mathsf{GS}} = 4$ iterations for both cases.
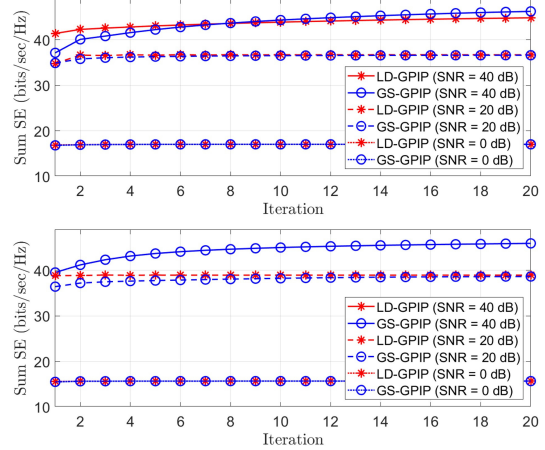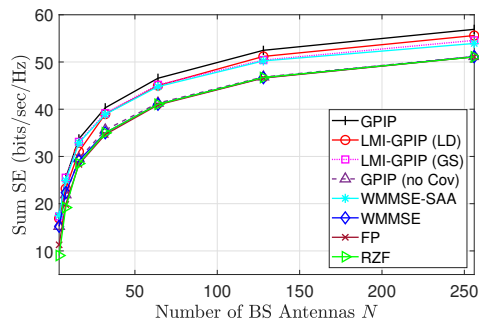

Fig. 2. The convergence behavior of the proposed algorithms for $N = 64$ BS antennas, $K = 4$ users, and SNR = $\{0, 20, 40\}$ dB.

Under the same environment as Fig. 1, Table II presents computation time results at SNR = 30 dB. Our findings confirm that our proposed algorithms significantly outperform GPIP in computation time. The simulation results demonstrate that both proposed algorithms maintain the comparable SE performance to GPIP with greatly reduced complexity. Compared to the baselines, Table II shows that the proposed algorithms achieve significantly faster execution than WMMSE-SAA while delivering superior SE performance over WMMSE and FP. In this regard, for lower-rank channels, LD-GPIP can be adopted with small r, resulting in fast execution with similar performance to GPIP. In contrast, GS-GPIP is preferable to maintain comparable performance to GPIP across any channel condition, albeit with a slight increase in computation time compared to LD-GPIP with small r.
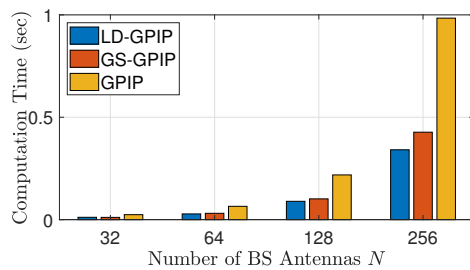
To identify the convergence characteristics of the proposed algorithms, we evaluate their performance with $N = 64$, $K = 4$, and SNR = $\{0, 20, 40\}$ dB. In the simulations, as stated in Fig. 1, we consider the two cases: low-rank channels (top), and high-rank channels (bottom). Fig. 2 shows that the proposed algorithms converge within 20 iterations across all SNR regimes. The results emphasize that the proposed algorithms demonstrate fast convergence.

We investigate our proposed algorithms in terms of the number of BS antennas. In this simulation, we consider SNR = 30 dB, $K = 4$, and $\Delta_k = \pi/12$. For each k, let the eigenvalues of $\boldsymbol{\Psi}_k$ be arranged in descending order as $|\lambda_{1,k}| \geq |\lambda_{2,k}| \geq \cdots \geq |\lambda_{N,k}|$. We then define the set of indices corresponding to eigenvalues that are at least 50% of the maximum as $\mathcal{S}_k = \left\{i \in \{1, \ldots, N\} \mid |\lambda_{i,k}| \geq 0.5\,|\lambda_{1,k}|\right\}$. Considering $r_k = |\mathcal{S}_k|$, we average these r_k values across all k, i.e., $\lceil \frac{1}{K}\sum_{k=1}^{K} r_k \rceil = r$. Fig. 3(a) shows that GPI-based algorithms consistently demonstrate superior sum SE performance across all N regimes. As shown in Fig. 3, LD-GPIP and GS-GPIP achieve the comparable SE performance to GPIP while reducing computation time. Moreover, we can conjecture from Fig. 3(b) that the complexity gains of the proposed algorithms become more prominent while achieving similar SE performance, which aligns with our intuition.

We evaluate the proposed algorithms with respect to the

This article has been accepted for publication in IEEE Transactions on Vehicular Technology. This is the author's version which has not been fully edited and content may change prior to final publication. Citation information: DOI 10.1109/TVT.2025.3644169

6
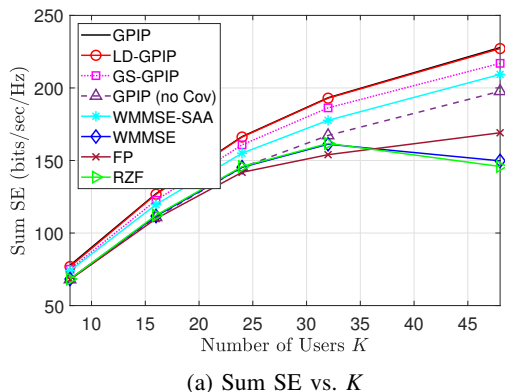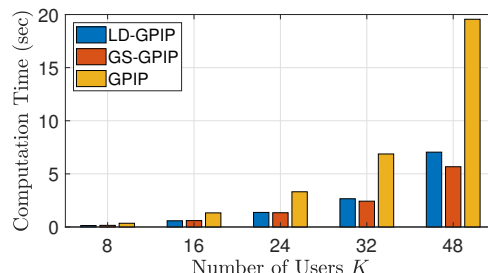
(a) Sum SE vs. N

(b) Computation Time vs. N

Fig. 3. The sum SE (a) and computation time (b) versus the number of BS antennas N for SNR = 30 dB and $K = 4$ users.

(a) Sum SE vs. K

(b) Computation Time vs. K

Fig. 4. The sum SE (a) and computation time (b) versus the number of users K for $N = 64$ BS antennas and SNR = 30 dB.

number of users for SNR = 30 dB, $N = 64$, $\Delta_k = \pi/12$, and setting r by the same $\geq 50\%$ eigenvalue rule as above. Fig. 4(a), shows GPIP-based methods outperform the baselines across K. LD-GPIP essentially matches GPIP, while GS-GPIP is slightly below (the gap can shrink with larger T_{GS}). Fig. 4(b) shows a runtime crossover: LD-GPIP is faster for $K \leq 24$, whereas GS-GPIP becomes faster for $K \geq 32$. This result aligns with our insight because LD-GPIP exhibits $O(K^3)$

complexity with respect to K, which is more affected by K compared with GS-GPIP. Hence, GS-GPIP is preferable in large-user scenarios, offering $O(N^2)$ complexity in N.

V. CONCLUSION

In this paper, we proposed the computationally efficient GPIP methods for massive MIMO systems with imperfect CSIT. By leveraging the block-diagonality of the GPI matrix, we applied the matrix inversion lemma for indirect computation of each sub-matrix inversion with low-rank approximation of channel estimation error matrices and the Gauss-Seidel method to achieve low-complexity matrix inversion. The proposed methods reduce complexity from $O(N^3)$ to $O(N^2)$ with respect to the number of BS antennas N. The numerical results demonstrated that both approaches achieve comparable SE performance to GPIP while significantly reducing computational overhead, rendering them practical solutions for massive MIMO systems. Moreover, our analysis revealed that the proposed methods are complementary in nature and can be adaptively utilized depending on the channel conditions.

REFERENCES

[1] J. Jeon, G. Lee, A. A. Ibrahim, J. Yuan, G. Xu, J. Cho, E. Onggosanusi, Y. Kim, J. Lee, and J. C. Zhang, "MIMO evolution toward 6G: Modular massive MIMO in low-frequency bands," *IEEE Commun. Mag.*, vol. 59, no. 11, pp. 52–58, 2021.

[2] M. A. Albreem, A. H. Al Habbash, A. M. Abu-Hudrouss, and S. S. Ikki, "Overview of precoding techniques for massive MIMO," *IEEE Access*, vol. 9, pp. 60 764–60 801, 2021.

[3] Q. Shi, M. Razaviyayn, Z.-Q. Luo, and C. He, "An iteratively weighted MMSE approach to distributed sum-utility maximization for a MIMO interfering broadcast channel," *IEEE Trans. Signal Process.*, vol. 59, no. 9, pp. 4331–4340, 2011.

[4] J. Choi, N. Lee, S.-N. Hong, and G. Caire, "Joint user selection, power allocation, and precoding design with imperfect CSIT for multi-cell MU-MIMO downlink systems," *IEEE Trans. Wireless Commun.*, vol. 19, no. 1, pp. 162–176, 2019.

[5] J. Wang, M. Bengtsson, B. Ottersten, and D. P. Palomar, "Robust MIMO precoding for several classes of channel uncertainty," *IEEE Trans. Signal Process.*, vol. 61, no. 12, pp. 3056–3070, 2013.

[6] H. Joudeh and B. Clerckx, "Sum-rate maximization for linearly precoded downlink multiuser MISO systems with partial CSIT: A rate-splitting approach," *IEEE Trans. Commun.*, vol. 64, no. 11, pp. 4847–4861, 2016.

[7] J. Choi, J. Park, and N. Lee, "Energy efficiency maximization precoding for quantized massive MIMO systems," *IEEE Trans. Wireless Commun.*, vol. 21, no. 9, pp. 6803–6817, 2022.

[8] M. Oh, J. Park, and J. Choi, "Joint optimization for secure and reliable communications in finite blocklength regime," *IEEE Trans. Wireless Commun.*, vol. 22, no. 12, pp. 9457–9472, 2023.

[9] S. Berra, A. Benchabane, S. Chakraborty, K. Maruta, R. Dinis, and M. Beko, "A Low Complexity Linear Precoding Method for Extremely Large-Scale MIMO Systems," *IEEE Open Jour, of Veh. Technol.*, 2024.

[10] B. Xu, Z. Wang, H. Xiao, J. Zhang, B. Ai, and D. W. K. Ng, "Low-complexity precoding for extremely large-scale MIMO over non-stationary channels," in *Proc. IEEE Int. Conf. Comm.* IEEE, 2023, pp. 6516–6522.

[11] C. Eckart and G. Young, "The approximation of one matrix by another of lower rank," *Psychometrika*, vol. 1, no. 3, pp. 211–218, 1936.

[12] C. F. Van Loan and G. Golub, "Matrix computations," *Johns Hopkins University Press, 3rd edition*, 1996.

[13] Y. Saad, *Iterative methods for sparse linear systems*. SIAM, 2003.

[14] K. Shen and W. Yu, "Fractional programming for communication systems—Part I: Power control and beamforming," *IEEE Trans. Signal Process.*, vol. 66, no. 10, pp. 2616–2630, 2018.

[15] A. Adhikary, J. Nam, J.-Y. Ahn, and G. Caire, "Joint spatial division and multiplexing—The large-scale array regime," *IEEE Trans. Inf. Theory*, vol. 59, no. 10, pp. 6441–6463, 2013.

[16] H. Yin, D. Gesbert, M. Filippou, and Y. Liu, "A coordinated approach to channel estimation in large-scale multiple-antenna systems," *IEEE J. Sel. Areas Commun.*, vol. 31, no. 2, pp. 264–273, 2013.